Journal of Applied Polymer Science

One-Pot Method for Obtaining Hydrophilic Tetracycline-Imprinted Particles via Precipitation Polymerization in Ethanol

Chunyan Zhao,[1,2] Jiangdong Dai,[3] Zhiping Zhou,[3] Xiaohui Dai,[1] Yongli Zou,[1,2] Ping Yu,[4] Tianbian Zou,[3] Chunxiang Li,[1] Yongsheng Yan[1]

[1]School of Chemistry and Chemical Engineering, Jiangsu University, Zhenjiang 212013, China
[2]School of the Environment and Safety Engineering, Jiangsu University, Zhenjiang 212013, China
[3]School of Material Science and Engineering, Jiangsu University, Zhenjiang 212013, China
[4]School of Computer Science, Jilin Normal University, 1301 Haifeng Street, Siping 136000, China
Correspondence to: Y. Yan (E-mail: zhaochunyan134@126.com)

ABSTRACT: In this study, we used a green, one-pot method to synthesize hydrophilic molecularly imprinted polymers (MIPs) via the precipitation polymerization of hydrophilic monomers in ethanol. The as-prepared materials were characterized by Fourier transform infrared spectroscopy, scanning electron microscopy, dynamic light scattering, and water contact angle measurements ($27.3 \pm 0.1^\circ$). As compared to the imprinting and nonimprinting processes, tetracycline (TC), as a template molecule, had an important effect on the morphology of the MIPs, and the possible mechanism is discussed in detail. We also discuss the effects of the parameters on the binding performance as determined by batch adsorption experiments in pure water. The adsorption capacity increased with increasing concentration and temperature at an optimum pH of 5.0. The Langmuir isotherm fitted the data better, with a maximal concentration of 45.75 μmol/g at 318 K. The kinetic properties of the MIPs (within 3.0 h) toward TC were analyzed with pseudo-first-order and pseudo-second-order kinetic equations and the intraparticle diffusion model. The MIPs exhibited specific recognition toward TC, and other competitive antibiotics were used as references. All of the results indicate that the MIPs exhibited a large adsorption capacity and great specific recognition for TC. The high affinity to TC of the MIPs, with its fast and easy fabrication, provides them with potential applications in the selective separation of the TC antibiotics from an aqueous environment. © 2013 Wiley Periodicals, Inc. J. Appl. Polym. Sci. **2014**, *131*, 40071

KEYWORDS: adsorption; molecular recognition; properties and characterization; radical polymerization; separation techniques

Received 20 May 2013; accepted 16 October 2013
DOI: 10.1002/app.40071

INTRODUCTION

Tetracycline (TC) antibiotics are used extensively as human and veterinary pharmaceuticals for the prevention and treatment of several infectious diseases and as feed additives to promote animal growth because of their broad spectrum antimicrobial activity and low cost.[1] However, most TCs in feed are unmetabolized and excreted via waste with only small fractions being absorbed by humans and animals.[2] In addition, these antibiotics are ubiquitous in aquatic and soil environments via the disposal of expired pharmaceuticals and domestic wastewater effluent; they present a threat to the ecosystem, including chronic and acute toxicity and microorganism antibiotic resistance within low-level exposure,[3,4] and eventually to humans through drinking water and the food chain.[5,6] Thus, the risk assessment of antibiotics has attracted significant research attention to date. Several studies have reported the occurrence of TCs in various countries.[7,8] However, the removal of TCs with conventional treatment methods is incomplete and limited, especially at trace concentrations. The development of a more effective and sensitive method for removing pharmaceutical antibiotics is thus of great importance.

The adsorption of high-binding sorbents is one of the most efficient processes for the elimination of contaminant compounds. So far, because of their high selectivity, low cost, easy preparation, and reusability, molecularly imprinted polymers (MIPs) have been widely used as selective adsorbents for the detection and separation of antibiotics, especially from complicated interfering substances.[9–12] They provide a potential route for collection and recycling. As is known, molecular imprinting, as a synthetically efficient route, has a reputation of creating

Additional Supporting Information may be found in the online version of this article.

artificial sites that are capable of target recognition. The route is an imprinting process via self-assembly between target molecules and functional monomers to form the complex, followed by copolymerization with a crosslinker. Binding cavities within the three-dimensional polymeric matrix after removal of the template exhibit a high specificity to the template and structurally related molecules.

Traditionally, MIPs are prepared via bulk polymerization as a porous monolith, and then, they have to be crushed, ground, and sieved into the desired particles, which are irregular in size and shape. The time-consuming process typically yields less than 50% and always destroys some recognition sites. Recently, alternative methods have been developed to address some of these issues; these include suspension polymerization,[13] emulsion polymerization, multistep polymerization,[14] and precipitation polymerization.[15,16] Of these techniques, precipitation polymerization, as a simple and attractive method, was used to prepare crosslinked imprinted conglobated microspheres in good yields; this involves polymerization in dilute solution (near-θ solvent) without an interfering reagent (surfactant or stabilizer), which can remain on the particles, and can potentially affect selective rebinding toward the template. In the mechanism, the entropic precipitation of nanogel particles and the continuous capture of oligomers from solution has conventionally predominantly resulted in the formation and growth of polymer microspheres.[17] The application of precipitation polymerization to molecular imprinting has afforded high-quality imprinted microspherical/nanospherical particles, which have been applied in liquid chromatography,[18] capillary electrochromatography,[19] solid-phase extraction,[20] and sensors.[21,22] However, current methods used to fabricate MIPs via precipitation polymerization are mostly performed in organic solvents, such as acetonitrile, dimethyl sulfoxide, and toluene, and thus do not meet the demands of green chemistry, that is, the design, development, and implementation of chemical products and processes to reduce or eliminate the use and generation of substances hazardous to human health and the environment.[23] Therefore, it is greatly necessary to develop and apply green polymerization techniques to prepare MIPs.

Despite the tremendous progress made in MIPs, the imprinting of hydrophilic compounds and specific template bindings in pure aqueous media, as one of the greatest challenges, significantly limits their practical applications and still remain to be addressed. An alternative strategy has been developed for the synthesis of water-compatible MIPs with molecular recognition performance in aqueous media; this involves the use of a hydrophilic comonomer, functional monomer, or crosslinker in the molecular imprinting process to improve the hydrophilicity.[24–26] The method is relatively simple in principle compared with the postmodification of the preformed MIPs.

To date, several studies on the preparation of MIPs with TC as the template molecule have been reported;[27–29] these MIPs have mainly been synthesized via bulk polymerization in hazardous solvents and have failed to be used in a pure water solution with low specific adsorption capacities because of their nonspecific hydrophobically driven binding. Hence, in this study, we developed a facile and green method for the preparation of water-compatible MIPs, namely, precipitation polymerization with TC as the target molecule, acrylamide (AAm) and methacrylic acid (MAA) as doubled functional monomers, and *N,N*-methylene bisacrylamide (MBAA) as a crosslinker. This system was carried out in the presence of a large amount of a green solvent, ethanol ($\geq$98% of the total mass), with azobisisobutyronitrile (AIBN) as an initiator. The as-obtained MIPs and molecularly nonimprinted polymers (NIPs) were then characterized with Fourier transform infrared (FTIR) spectroscopy, scanning electron microscopy (SEM), dynamic light scattering (DLS), and static contact angle and water dispersion experiments. The equilibrium and kinetic binding properties were investigated in detail. We also discussed the effects of different parameters, including the solution pH, solvent, initial concentration, temperature, and contact time, on the binding ability. Furthermore, selective rebinding experiments were carried out to demonstrate the specific recognition of MIPs toward the template, whereas other competitive antibiotics were used as references.

EXPERIMENTAL

Materials

MAA (Aladdin) was purified by distillation under reduced pressure. AAm and AIBN were purchased from Sinopharm Chemical Reagent Co., Ltd. (Shanghai, China) and purified through recrystallization in acetone and ethanol, respectively. TC, sulfamethazine (SMZ), cefalexin (CFX), chlortetracycline (CTC), ciprofloxacin (CIP), HCl, $NH_3{\cdot}H_2O$, acetic acid, ethanol, and MBAA (analytical grade) were purchased from Aladdin Reagent Co., Ltd. (Shanghai, China), and were used as received. Double-distilled water was purified with a Purelab Ultra system (Organo, Tokyo, Japan).

Synthesis of the MIPs

The MIPs were synthesized via precipitation polymerization according to the literature with some modifications. In a brief process, the optimal recipe for the total amount of monomer(s) was 2.0 g of AAm/MAA/MBAA (3.0:1.0:0.48 mol/mol), 0.1 g of AIBN, 95 g of ethanol, and 30 mg of TC. Self-assembly between the functional monomers and template molecules was performed in a 250-mL, three-necked, round-bottomed flask at room temperature in the dark for 12 h. The mixing solution was purged with nitrogen for 10 min while it was cooled in an ice bath. The initiator solution (0.1 g/5.0 g of ethanol) was injected into the flask while the temperature was heated to the settled temperature (60°C). Batch polymerization was used for 14 h with an agitation rate of 300 rpm. The resulting polymers were separated from the mixed solution by centrifugation and were then washed with ethanol to remove the adsorbed oligomers and unreacted monomers. The products were then washed repeatedly with a mixture of methanol and acetic acid (9:1 v/v) to extract the embedded template in a Soxhlet extractor until no TC was detected in the supernatant with an ultraviolet–visible (UV–vis) spectrophotometer at 275.8 nm. For comparison, the NIPs were synthesized under the same chemical conditions, except with the absence of the template TC.

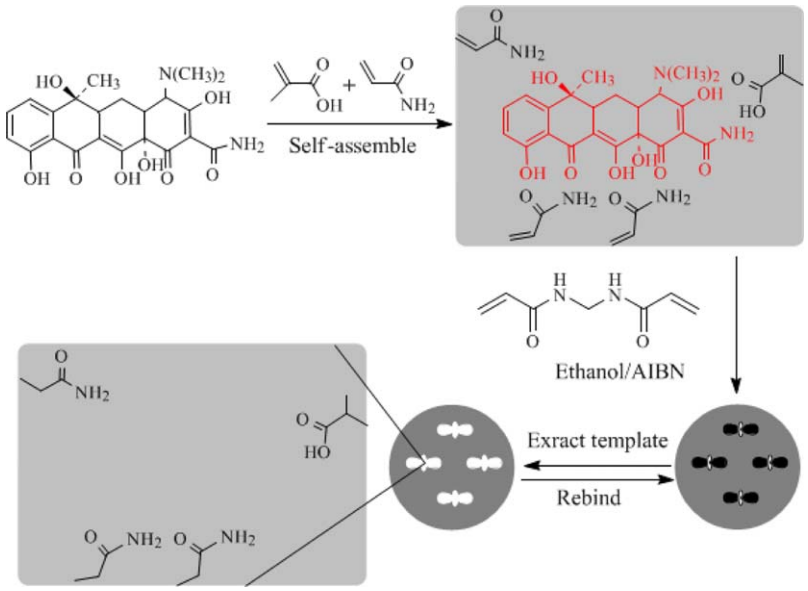

Figure 1. Schematic illustration of a possible mechanism for the imprinting process. [Color figure can be viewed in the online issue, which is available at wileyonlinelibrary.com.]

Measurements of Molecular Recognition Properties

Batch adsorption experiments were performed to study the effects of the experimental parameters on the separation of TC; these parameters included the pH, solvent, initial concentration, temperature, and contact time. After adsorption, the mixture solution was isolated by centrifugation, and the supernatants were then filtered with a 0.22-μm filter membrane and examined with the UV–vis spectrophotometer at λ_{max} (λ_{max} was the corresponding wavelength of maximum absorption peak in the absorption spectra) of 275.8 nm. The amounts of TC adsorbed at equilibrium (Q_e; μmol/g) and at time t (Q_t; μmol/g) were calculated according to the following equations, respectively:

$$Q_e = \frac{(C_0 - C_e)V}{m} \quad (1)$$

$$Q_t = \frac{(C_0 - C_t)V}{m} \quad (2)$$

where C_0, C_t, and C_e (μmol/L) are the concentrations at the initial time, time t, and equilibrium of the TC solution, respectively; V is the volume of the TC solution; and m is the weight of the adsorbent.

To determine the selective recognition of the MIPs with TC-imprinted cavities for the template molecule, 5.0 mg of the MIPs/NIPs were added to 10-mL test tubes containing 10 mL of aqueous solution with 100 μmol/L TC, CTC, CIP, CFX, and SMZ, respectively. Moreover, the competitive adsorption of the MIPs/NIPs for TC in the presence of 100 μmol/L CTC, CIP, CFX, and SMZ was investigated. The pH of the initial solution was not adjusted, and static experiments were carried out in a water bath at 25°C for 12 h. After adsorption, the mixture was filtered with a 0.22-mm membrane. The free TC concentrations were measured with an Agilent 1200 high-performance liquid chromatography (HPLC) system with a UV–vis detector. The mixture solvent of methanol and water (pH 3; 70:30 v/v) was used as the mobile phase at a 1.0 mL/min flow rate. The injection loop volume was 20 μL, and the oven temperature was set at 25°C.

Characterization

Infrared spectra were recorded on a Nicolet NEXUS-470 spectrophotometer with KBr pellets. The morphologies, particle sizes, and size distributions of the samples were observed by field emission SEM (S-4800). The SEM size data calculated reflected an average of all of the particles in the SEM images.

The polymer thin films of the MIPs and NIPs were prepared by the casting of their dispersion solutions in ethanol (15 mg/mL, after ultrasonic dispersion) on clean glass surfaces. After the solvent was allowed to evaporate at ambient temperature overnight, a KSV CM200 contact angle instrument (Finland) was used to determine their static water contact angles. Two measurements were taken for each sample, with their average being used for analysis.

The suspensions of the MIPs and NIPs in pure water (1.0 mg/mL) were first dispersed by ultrasonication, and they were then allowed to settle down for different times at 25°C to check their dispersion stability.

DLS measurements were performed in a thermostated bath regulated at 25°C on a Bettersize 2000 apparatus (Dandong Baite Instrument Co., China), and we recorded the autocorrelation functions.

A PHS-2 acidometer (Second Analytical Instrument Factory of Shanghai, China) was used for pH measurements.

RESULTS AND DISCUSSION

Mechanism of Imprinted Polymerization in Ethanol

The aim of this study was to develop a facile, general, and efficient approach for obtaining hydrophilic imprinted polymers. According to the Ni and Kawaguchi's[30] research, a new mechanism was used to explain the microsphere formation via the

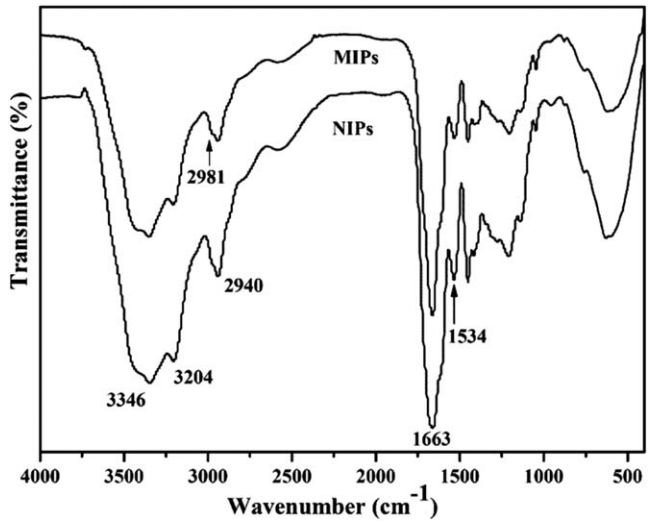

Figure 2. FTIR spectra of the MIPs and NIPs.

precipitation polymerization of AAm/MAA in ethanol. Figure 1 shows the possible mechanism of the imprinting process. When the temperature increased to 60°C, complexes of AAm/MAA/MBAA formed as minimonomer droplets because of hydrophobic interactions and presumably decreased the solubility in ethanol. The nonimprinted microspheres originated from polymerization in the minimonomer droplets, triggered by both the oligoradicals captured and the partitioned initiator molecules. The growth of the microspheres depended on monomer transfer to the growing microspheres via the incorporation of minimonomer droplets, which naturally affected the final number and morphologies of the microspheres. When the TC molecule used as the template was added to the polymerization system, hydrogen-bonding and electrostatic interactions mainly formed between the TC molecules and functional monomers. As a result, the structure of the AAm–MAA–MBAA complexes might have been destroyed; this led to a complicated reaction, as expected.

Characterization of the MIPs

Figure 2 shows the FTIR spectra of the MIPs and NIPs, which were used to assess the chemical composition of the two polymers. The broad characteristic peaks between 3346 and 3204 cm^{-1} were assigned to secondary amide N—H stretching vibrations. The signals at 2981 and 2940 cm^{-1} were attributed to —CH_3 and —CH_2 stretching vibrations, respectively. Deformation vibrations of N—H produced the signal at 1534 cm^{-1}. The characteristic peak of the carboxyl from the MAA monomer did not obviously occur but may have be overlapped with the

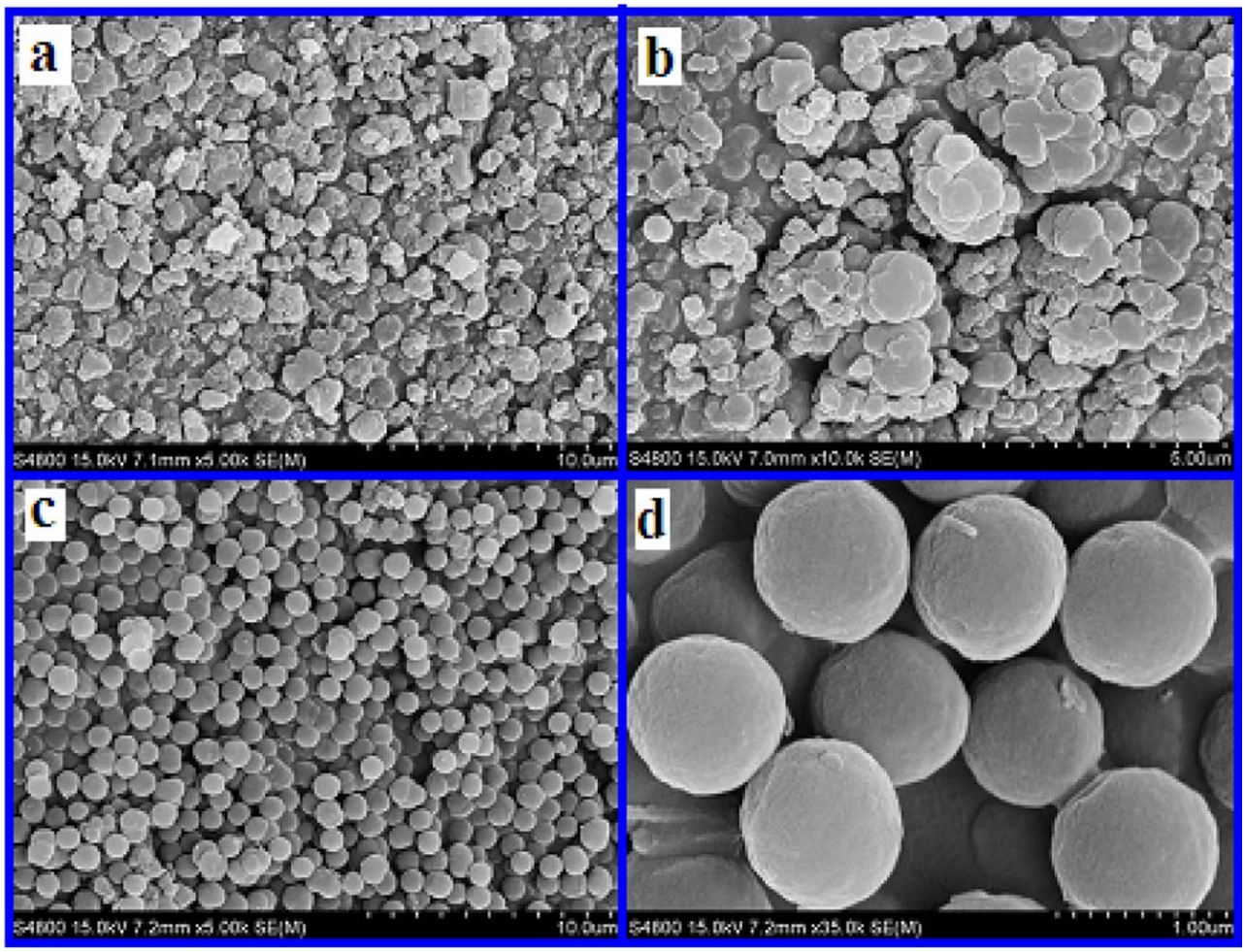

Figure 3. SEM images of the (a,b) MIPs and (c,d) NIPs. [Color figure can be viewed in the online issue, which is available at wileyonlinelibrary.com.]

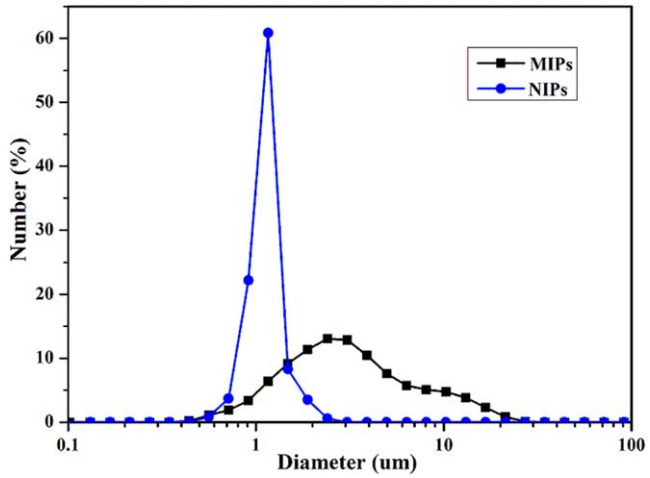

Figure 4. Size distributions calculated from the DLS measurements for the MIPs and NIPs dispersed in pure water. [Color figure can be viewed in the online issue, which is available at wileyonlinelibrary.com.]

secondary amide C═O stretching; instead, a sharp peak was observed at 1663 cm^{-1}. The previous results showed that all of the monomers successfully participated in the polymerization.

Field emission SEM was used to observe the morphology of the MIPs and NIPs. Figure 3(a,b) shows that the molecularly imprinted microparticles were irregular and crosslinked agglomerates with a size ranging from 0.8 to 2.5 μm. It was clear that the MIPs were uniformly spherical and monodisperse with an average size of around 1.0 μm [Figure 3(c,d)]. The addition of the template TC evidently affected the interaction between MAA and AAm so that the morphology changed enormously from a spherical shape to irregular particles.

DLS was used to measure the particle size distribution of the MIPs and NIPs, and the data calculated are shown in Figure 4. The main peak of the particle size distribution for the NIPs was found between 0.7 and 1.1 μm; they also showed a relatively small polydispersity. However, the agglomerate size distribution for the MIPs was greatly broad and matched the result of the SEM images well.

The hydrophilicity of the MIPs and NIPs was accurately evaluated by performing static water contact angle experiments. Figure 5(a,b) showed the profiles of a water drop on the MIPs and NIPs films, from which the static water contact angles were determined to be $27.3 \pm 0.1°$ and $27.8 \pm 0.2°$ for MIPs and NIPs, respectively. The results clearly showed that the MIPs and NIPs films exhibited significantly higher hydrophilicity. The use of hydrophilic monomers has proven to be highly efficient for improving the dispersion stability of the materials in water. Therefore, we expected that the MIPs and NIPs would show an enhanced dispersion stability in water at ambient temperature; this is demonstrated in the results shown in Figure 5(c).

Effect of the Solvent

The solvent played an important role in the binding because of the competing affinity to TC. The solute TC was dissolved in the different solvents, where the water-containing ethanol at 0, 50, and 100% formed 50, 80, and 100 μmol/L TC solutions, respectively. As shown in Figure 6, when the solution was 100% water, the adsorption amounts of TC on the MIPs and NIPs were both high in the three concentrations; this indicated that nonspecific adsorption occurred in the NIPs. However, the high adsorption amount of TC on the MIPs in pure water was mainly attributed to the electrostatic and hydrophobic interactions and the size and structural complementarity between the TC and MIPs. With the volume of ethanol halved, the nonspecific binding decreased greatly for the NIPs, and the specific binding of TC on the MIPs also rapidly decreased; this was attributed to the intermediate polarity of the MIPs with respect to the solvents used. The hydrogen-bonding interaction between the TC and MIPs became the main interaction force in pure ethanol, and the adsorption capacity of TC on the MIPs increased. Figure 6 also demonstrates that the selectivity of the MIPs was maintained in an aqueous medium, although it had nonspecific adsorption onto the polymer. Thus, the application of MIPs under aqueous conditions was possible.

Effect of the Solution pH

To investigate the effect of the pH (as an important controlling parameter) in the adsorption and separation of TC from the aqueous medium, 5.0 mg of sorbent (MIPs or NIPs) was dispersed in 10 mL of 80 μmol/L solutions with various initial pHs at 298 K for 12 h; the solutions were adjusted by spots of 0.1*M* HCl and 0.1*M* $NH_3 \cdot H_2O$ solutions. Because TC was

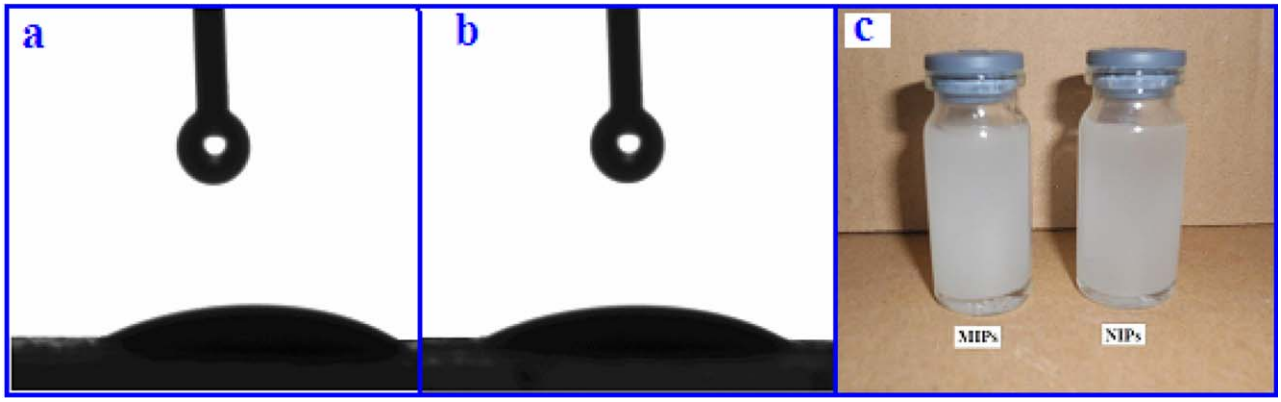

Figure 5. Profiles of the water drops on the (a) MIP and (b) NIP films and (c) photograph of the dispersion of the MIPs and NIPs in pure water (1.0 mg/mL) at 25°C. [Color figure can be viewed in the online issue, which is available at wileyonlinelibrary.com.]

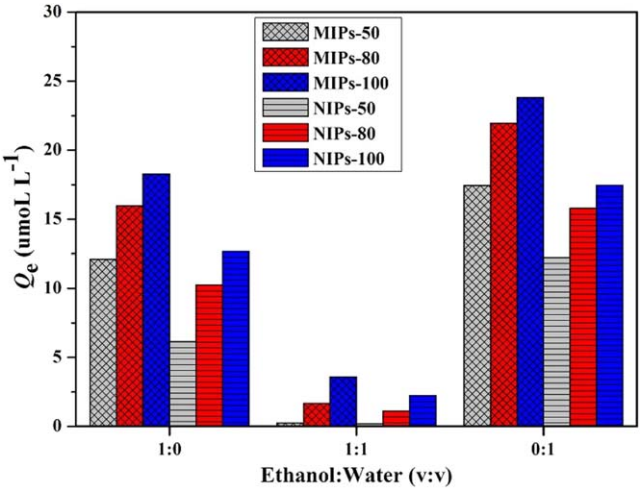

Figure 6. Adsorption of TC on the MIPs and NIPs in ethanol–water solutions with different proportions and TC concentrations. [Color figure can be viewed in the online issue, which is available at wileyonlinelibrary.com.]

degraded when the pH was lower than 2.0 and over 7.0, the effect of pH was analyzed in the range of pH of 3.0–7.0. After the adsorption was completed, the final pH was also measured, and the variation was all within 1.0 pH unit.

The tetracycline hydrochloride used had several ionizable groups, including the acidic hydroxyl groups (at C-3, $pK_a = 3.30$, and C-10, $pK_a = 7.68$) and dimethylamino groups (at C-4, $pK_a = 9.69$).[31] With the change in pH, TC may have existed in the solution as positively and/or negatively charged species. TC occurred either as a zwitterion or a cation in the pH 4.0 solution or as anionic ion in the pH 6.0 and 7.0 solutions. However, in the pH 5.0 solution, TC was predominantly neutral with an internal zwitterion of dimethylamino groups protonated and the hydroxyl group ionized (at C-3). It was obvious that the maximum value of the adsorption capacity for the MIPs was present at pH 5.0 (Figure 7); this suggested that TC in the zwitterion form was more favorable for adsorption onto the MIPs better than TC in the cationic or anionic form. As shown, there was a significant difference in the adsorption amount to TC obtained from the MIPs and that from the NIPs; this suggested the selective adsorption for the MIPs to TC at every pH studied. Furthermore, the pH value of the TC solution without adjustment was approximately 5.0 in our study. Therefore, pH 5.0 was selected for the following experiments.

Effects of the Initial Concentration and Temperature

To study the effects of the initial concentration and temperature, 5.0 mg of adsorbents (MIPs and NIPs) were placed into 10-mL TC solutions with initial concentrations ranging from 10 to 200 μmol/L at 298–318 K for 12 h. As shown in Figure 8, it was clear that the adsorption capacities of the MIPs and NIPs toward TC increased with increasing TC concentration; this provided the necessary driving force to overcome the resistances to the mass transfer of TC between the aqueous and solid phases. The adsorption capacity of TC onto the MIPs and NIPs was found to increase with increasing temperature from 298 to 318 K; this also had a significant influence on the adsorption process and indicated that the process was endothermic in nature. Meanwhile, the adsorption capacity of TC onto the MIPs was much larger than that onto the NIPs in the whole range of initial concentrations and temperatures [Figure 8(a,b)]; this suggested a good imprinting effect and selectivity for TC with the MIPs adsorbents.

Adsorption Isotherms

Isotherm models have been successfully applied to describe the adsorption process and investigate the mechanisms of adsorption. In this study, the Langmuir and Freundlich isotherms in linear form were used to analyze the adsorption equilibrium curves of TC on the obtained materials.

The Langmuir isotherm was valid for monolayer adsorption onto the materials with a finite number of identical binding sites. The linear form of the Langmuir equation can be expressed as follows:[32]

$$\frac{C_e}{Q_e} = \frac{C_e}{Q_m} + \frac{1}{K_L Q_m} \tag{3}$$

where Q_e is the adsorption capacity of TC at equilibrium (μmol/g), C_e is the free concentration of the TC solution at equilibrium (μmol/L), Q_m is the maximum adsorption amount (μmol/g), and K_L is the Langmuir constant (L/g).

Equilibrium parameter (R_L), as a dimensionless constant, was defined by Weber and Chakkravorti[33] to express the essential characteristics of the Langmuir isotherm, according to the following equation:

$$R_L = \frac{1}{1 + K_L C_0} \tag{4}$$

where K_L is the Langmuir constant (L/g) and C_0 is the initial concentration of the TC solution (μmol/L).

The R_L value indicates the shape of isotherm as follows: (1) when R_L is greater than 1, it is unfavorable; (2) when R_L is 1, it

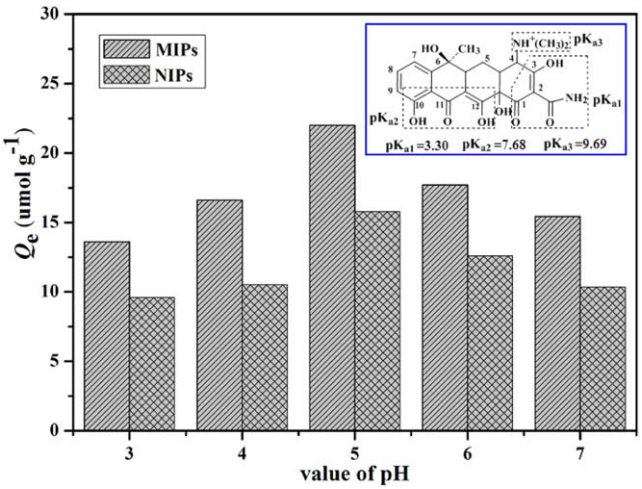

Figure 7. Effect of the pH on the adsorption of TC onto the MIPs and NIPs at 298 K. The chemical structure and pK_a values of the TC molecule are shown in the inset. [Color figure can be viewed in the online issue, which is available at wileyonlinelibrary.com.]

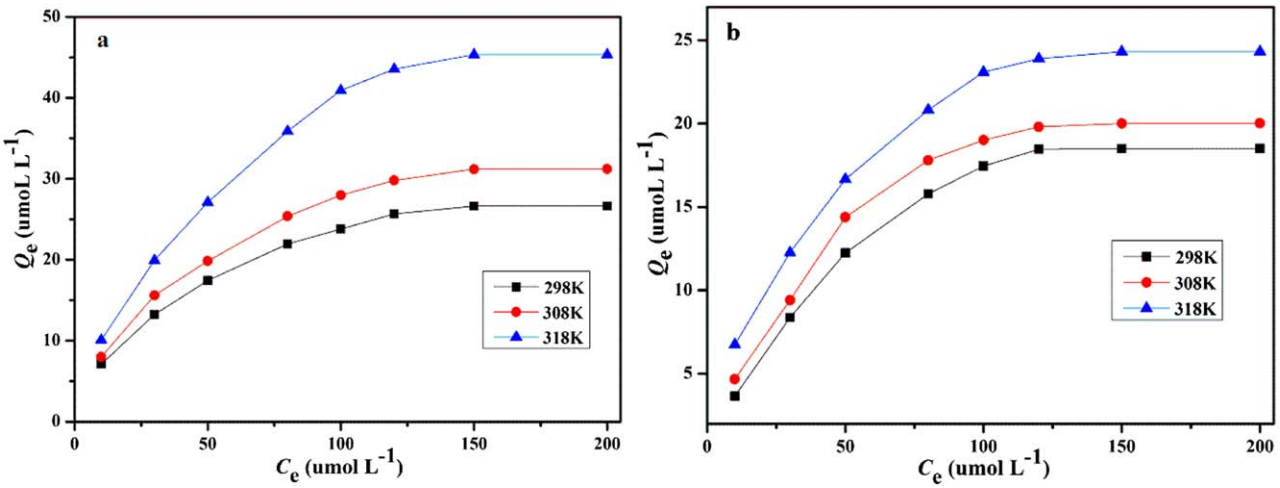

Figure 8. Effects of the temperature and initial concentration on the adsorption of TC onto the (a) MIPs and (b) NIPs. [Color figure can be viewed in the online issue, which is available at wileyonlinelibrary.com.]

is linear; (3) when 0 is less than R_L and R_L is less than 1, it is favorable; and (4) when R_L is 0, it is irreversible. The Langmuir plots for TC binding onto the MIPs and NIPs are shown in Figure 9, and the parameters are listed in Table I.

The values of Q_m for the MIPs and NIPs increased with increasing contact temperature; this indicated that the adsorption processes were endothermic. The correlation coefficients (R^2's) of the isotherms for both the MIPs and NIPs were all higher than 0.98 at the three temperatures; this indicated that the Langmuir isotherm fit the experimental data very well. This probably provided proof for monolayer adsorption on the surface of the polymers, predominated by chemical adsorption. Although the carboxyl and amide groups of the MIPs and NIPs were saturated with TC, the adsorption amount was difficult to increase further, and it reached equilibrium. As shown in Table I, all of the R_L values calculated were in the range 0.110–0.797; this confirmed that the adsorption of TC onto the as-prepared polymers was all favorable under the experimental conditions. Moreover, the R_L values gradually decreased with increasing initial concentration from 10 to 200 μmol/L. This indicated that the adsorption was more favorable at higher concentrations.

The Freundlich model is an empirical equation for sorption onto heterogeneous surfaces; it assumes that the stronger binding sites were occupied first and that the binding strength decreased with increasing degree of site occupation.[34] The linear Freundlich isotherm can be expressed as follows:

$$\ln Q_e = \ln K_F + \frac{1}{n} \ln C_e \quad (5)$$

where K_F [(μmol g^{-1})(L μmol^{-1})$^{1/n}$] and n are the Freundlich constants to be determined.

The Freundlich model was used in the adsorption process with the noncovalently imprinted polymers.[35] The Freundlich constants were calculated according to the slope and intercept in Figure 10 and are listed in Table I. In this study, the correlation coefficient ($R^2 > 0.93$) reflecting the experimental data also fit the Freundlich model relatively well, and the nonlinear isotherms were attributed to the adsorption site heterogeneity, hydrogen-bonding interactions, electrostatic attraction, and other interactions. The values of $1/n$ for the MIPs and NIPs at the three temperatures were all smaller than 1.0; this was favorable for the removal of TC from an aqueous solution.

Adsorption Kinetics

The effect of the contact time on the adsorption of TC is shown in Figure 9. The amount of TC adsorbed onto the MIPs and NIPs increased with increasing contact time. The rapid adsorption observed for the MIPs within the first 180 min was probably due to the abundant availability of imprinted cavities, and finally, equilibrium was established. The adsorption for NIPs toward TC achieved saturation after 120 min; this may have been caused by the occupancy of active sites on the polymer surface. We noted that the adsorption amount of MIPs for TC reached 21.931 μmol/g after 4.0 h of contact; this was higher than the 15.459 μmol/g of the NIPs and demonstrated the good imprinting effect of the MIPs.

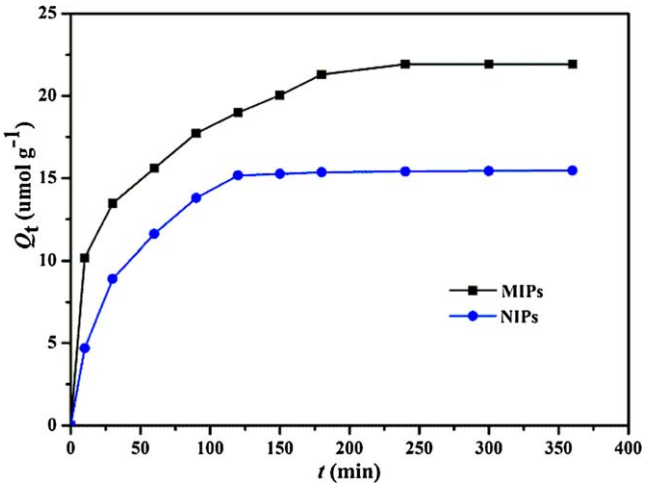

Figure 9. Effect of the contact time on the TC adsorption onto the MIPs and NIPs. [Color figure can be viewed in the online issue, which is available at wileyonlinelibrary.com.]

Table I. Fitting Parameters of the Langmuir and Freundlich Models for TC adsorption onto the MIPs and NIPs

			Langmuir				Freundlich		
Sorbents	Temperature (K)	$Q_{e,exp}$ (μmol/g)	Q_m (μmol/g)	K_L (L μmol^{-1})	R_L	R^2	K_F [(μmol/g) (L μmol^{-1})1/n]	1/n	R^2
MIPs	298	26.78	31.15	0.0344	0.732-0.120	0.9948	3.511	0.4159	0.9726
	308	31.27	36.36	0.0332	0.729-0.119	0.9946	4.093	0.4178	0.9735
	318	45.75	53.76	0.0350	0.741-0.125	0.9904	5.200	0.4506	0.9747
NIPs	298	18.50	23.42	0.0254	0.797-0.164	0.9854	1.378	0.5400	0.9390
	308	20.02	24.04	0.0335	0.749-0.130	0.9899	2.019	0.4782	0.9337
	318	24.71	28.255	0.0405	0.712-0.110	0.9939	3.359	0.4099	0.9602

The kinetic parameters helped in the examination of the mechanism and rate-controlling step in the overall adsorption process. Different kinetic models were adopted to analyze the adsorption kinetics data, namely, the pseudo-first-order and pseudo-second-order kinetic equations and intraparticle diffusion.

The pseudo-first-order[36] and pseudo-second-order kinetic equations[37] are expressed as follows:

$$\ln(Q_e - Q_t) = \ln\ Q_e - k_1 t \tag{6}$$

$$\frac{t}{Q_t} = \frac{1}{k_2 Q_e^2} + \frac{1}{Q_e} t \tag{7}$$

where Q_e and Q_t are the amounts of TC adsorbed at equilibrium and at time t (μmol/g), respectively; k_1 is the pseudo-first-order rate constant (min^{-1}); and k_2 is a constant of the pseudo-second-order rate equation (g μmol^{-1} min^{-1}).

According to eq. (6), the values of the correlation coefficient (R^2) were relatively low (Table II). In addition, the experimental values of the amount of TC adsorbed at equilibrium ($Q_{e,exp}$'s) were far from the theoretical values calculated from the linear plots ($Q_{e,cal}$'s). The result suggest that the pseudo-first-order kinetic equation was not suitable for the adsorption process. However, the pseudo-second-order model fit the experimental data well (with $R^2 > 0.99$), and the $Q_{e,exp}$ and $Q_{e,cal}$ values were highly consistent; this indicated the utilization of the second-order kinetic model to describe the adsorption process well. The good fit supported the assumption that adsorption rate was controlled by chemical sorption,[38] which agreed with the possible interaction between TC and the obtained polymers.

As the previous models were not able to identify the diffusion mechanism of the adsorption process, the intraparticle diffusion model was proposed to test the experimental data and could be express as follows:[39]

$$Q_t = k_p t^{1/2} + C \tag{8}$$

where k_p is the intraparticle diffusion rate constant (μmol g^{-1} min$^{-1/2}$) and C is the intercept.

The adsorption of the target from solution essentially involved three consecutive steps. The initial step was the external surface or instantaneous adsorption. The adsorption gradually occurred in the second step, where intraparticle diffusion was rate-limiting. In the third step, the adsorption equilibrium reached the point where intraparticle diffusion started to slow down because of the extremely low free concentrations left in the solutions.[40] The intraparticle diffusion plot of Q_t versus $t^{1/2}$ ($t^{1/2}$ was time required for the adsorption to half equilibrium value) for the MIPs and NIPs are shown in Figure 10, with a double straight-line nature. Initially, we assumed that TC rapidly reached the external surface of the polymers through film diffusion. The first sharper region could be caused by the entry of the TC molecules into the polymer particles via intraparticle diffusion. Finally, the second linear region represented the equilibrium stage. The k_p value of the MIPs was lower than that of the NIPs; this may have been due to the existence of imprinted cavities in the MIPs, which took a longer time to accomplish the rebinding.

Investigation of the Selectivity Properties

As evident in Figure 11(a), we chose four typical antibiotics, including structurally analogous CTC and structurally different CFX, CIP, and SMZ to examine the molecular selectivity of TC-imprinted sites in the MIPs. The MIPs had the maximal adsorption amount for TC among the five antibiotics [Figure 11(b)]; it exhibited a high adsorption selectivity toward the template molecule with the hydrogen-bond interaction measured by ^{1}H-NMR (Fig. S1). This implied that the recognition of the MIPs

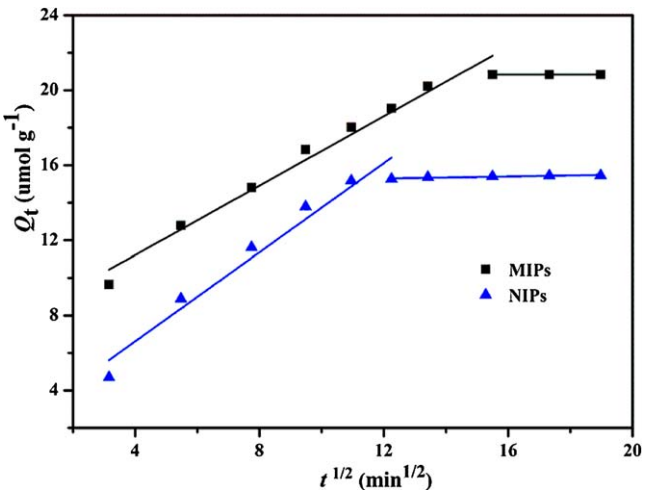

Figure 10. Intraparticle diffusion plots for the TC adsorption onto the MIPs and NIPs at 298 K. [Color figure can be viewed in the online issue, which is available at wileyonlinelibrary.com.]

Table II. Kinetic Parameters for TC Adsorption onto the MIPs and NIPs

Kinetic model	Parameter	MIPs	NIPs
Pseudo-first-order	$Q_{e,exp}$ (μmol/g)	21.93	15.46
	$Q_{e,cal}$ (μmol/g)	14.87	7.873
	k_1 (min^{-1})	0.016	0.0098
	R^2	0.9510	0.9336
Pseudo-second-order	$Q_{e,cal}$ (μmol/g)	23.202	16.502
	k_2 (g μmol^{-1} min^{-1})	0.00211	0.00231
	R^2	0.9996	0.9986
Intraparticle diffusion	k_p (μmol g^{-1} $min^{-1/2}$)	0.9251	1.3313
	R^2	0.9784	0.9868

was dominated not only by the interactions between the functional groups but also by the molecular size and structure of the adsorbates. The adsorption amount of the MIPs for CTC was just a little less than that for TC; this might have been to their similar chemical structures. Although the SMZ molecule was small enough to enter into the imprinting cavities but not perfectly matched, thus they had a lower chance to be captured by the MIPs. In addition, the difference of the adsorption amount between the MIPs and NIPs for each antibiotic suggested that the MIPs were specific to TC but nonspecific to other antibiotics. Also, the values of K_d (K_d was the distribution coefficient), k (k was the selectivity coefficient), and β (β was

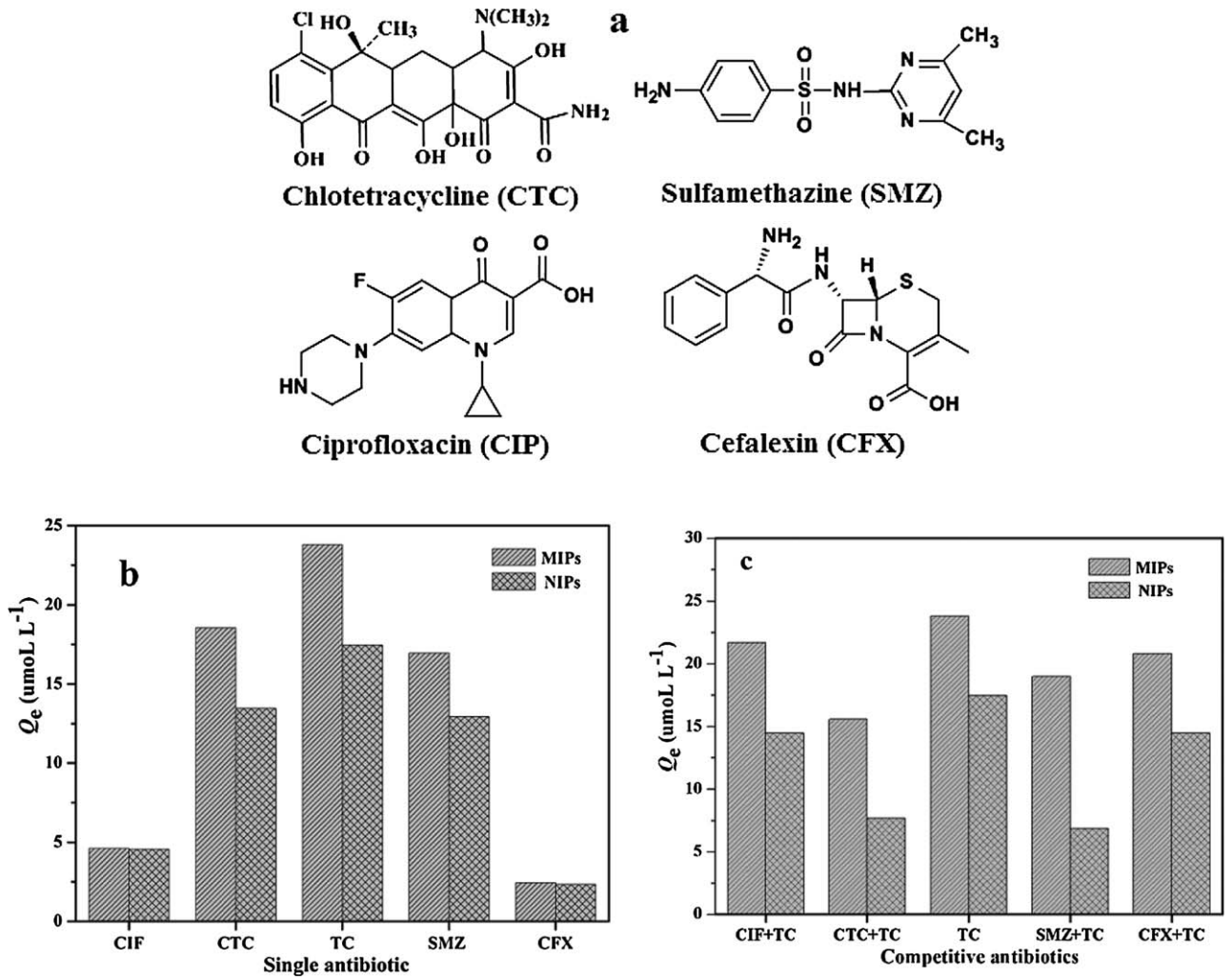

Figure 11. (a) Chemical structures of the competitive antibiotics and selective adsorption performance of the MIPs and NIPs toward TC in (b) single-antibiotic and (c) dual-antibiotic solutions.

the relative selectivity coefficient) values are summarized in Table S1 (see the Supporting Information), we drew the following results:

1. The values of k of the MIPs significantly increased compared to those of the NIPs; this suggested that the MIPs had the highest selective binding ability for TC.
2. The values of β showed the binding affinity of the recognition sites to the analytes. The values of β for CTC, CIP, SMZ, and CFX were 1.1128, 1.0319, 1.0723, and 0.9106, respectively. This indicated that the recognition for antibiotics followed the order CTC > SMZ > CIP > CFX.

All of the results illustrated the success of the imprinted process.

To further study the adsorption selectivity properties of the MIPs toward TC, four competitive antibiotics, including CTC, CIP, CFX, and SMZ, were suspended in a TC solution to determine the effects on TC adsorption. As shown in Figure 11(c), the MIPs exhibited high TC adsorption amounts in the existence of other antibiotics. As expected, the present of CTC affected the adsorption amount because of the extremely similar shape and structure. For the other three antibiotics, the TC–MIPs exhibited good selectivity to the template molecule in the competitive environment. However, the adsorption amounts of the NIPs toward TC sharply decreased in the double-antibiotic solutions. All of the results suggest that the TC-imprinted sites were successfully formed in the MIPs through precipitation polymerization in ethanol.

Comparison of these TC–MIPs with Those in Other Reports

Several researchers have published methods for the preparation of the MIPs with TC as the template. Generally, TC–MIPs have been prepared via bulk polymerization in toxic organic solvents, such as methanol, dimethyl sulfoxide, and acetonitrile,[27–29] with an irregular shape and size, and the procedure has been time-consuming. In addition, the prepared MIPs have shown a very low capacity and imprinting factor. A TC–MIP solid-phase microextraction fiber synthesized by Hu et al.[41] was used to analyze trace TCs in complicated samples, but the extraction capacity toward TC was only 100 ng. Moreover, most of the previous TC–MIPs have been hydrophobic and have exhibited good specific adsorption to TC in the pure water environments. However, in this study, precipitation polymerization was used to prepare the hydrophilic TC–MIPs in a green solvent (ethanol) without the addition of surfactant, and the process was simple and effective. The as-obtained material had a high adsorption capacity (45.336 μmol/g) and good selectivity to TC molecules in a water medium. We developed a simple method for achieving the selective recognition and separation of the target molecule in aqueous environmental samples.

CONCLUSIONS

In this article, we presented a facile and green method to synthesize water-compatible MIPs with TC as the target molecule. The polymerization was carried out in a nontoxic and cheap solvent, ethanol, the mechanism of which has been also discussed in detail. The results of the characterization with FTIR spectroscopy, SEM, DLS, and water contact angle measurements show that the polymer microparticles were hydrophilic with small contact angles, and the morphologies were greatly affected by the addition of TC molecules. The optimum value of the solution pH was 5.0 for adsorption of TC onto the MIPs and NIPs. Moreover, the MIPs exhibited a big adsorption capacity and specific affinity to the template molecule in the pure water, and the adsorption mounts increased with increasing initial concentration, reaction temperature, and contact time. The maximum adsorption capacities calculated by the Langmuir model for the MIPs were 26.780, 31.266, and 45.75 μmol/g at 298, 308, and 318 K, respectively. The MIPs reached adsorption equilibrium within 3.0 h. As compared with three other antibiotics (CFX, CIP, and SMZ), the MIPs exhibited a high adsorption selectivity toward the template molecule. In conclusion, the method used to synthesize water-compatible MIPs was available and effective. The prepared MIPs could potentially be applied to selectively separate TC antibiotics from an aqueous environment.

ACKNOWLEDGMENTS

This work was financially supported by the National Natural Science Foundation of China (contract grant numbers 21077046, 21004031, 21176107, 21174057, 21107037, and 21277063), the National Basic Research Program of China (973 Program, contract grant number 2012CB821500), and the Ph.D. Innovation Programs Foundation of Jiangsu Province (contract grant number CXZZ13_0668).

REFERENCES

1. Sören, T. B. *J. Plant Nutr. Soil Sci.* **2003**, *166*, 145.
2. Sarmah, A. K.; Meyer, M. T.; Boxall, A. B. A. *Chemosphere* **2006**, *65*, 725.
3. Boxall, A. B. A.; Kolpin, D. W.; Halling-Sorensen, B.; Tolls, J. *Environ. Sci. Technol.* **2003**, *37*, 286.
4. Schmitt, H.; Stoob, K.; Hamscher, G.; Smit, E.; Seinen, W. *Microb. Ecol.* **2006**, *51*, 267.
5. Lin, C. Y.; Huang, S. D. *Anal. Chim. Acta* **2008**, *612*, 37.
6. Maskaoui, K.; Hibberd, A.; Zhou, J. L. *Environ. Sci. Technol.* **2007**, *41*, 8038.
7. Hirsch, R.; Ternes, T. A.; Haberer, K.; Kratz, K. L. *Sci. Total Environ.* **1999**, *225*, 109.
8. Tolls, J. *Environ. Sci. Technol.* **2001**, *35*, 3397.
9. Aristilde, L.; Marichal, C.; Miéhé-Brendlé, J.; Lanson, B.; Charlet, L. *Environ. Sci. Technol.* **2010**, *44*, 7839.
10. Chen, W. R.; Huang, C. H. *Chemosphere* **2010**, *79*, 779.
11. Oleszczuk, P.; Pan, B.; Xing, B. S. *Environ. Sci. Technol.* **2009**, *43*, 9167.
12. Zhang, S. J.; Shao, T.; Karanfil, T. *Water Res.* **2011**, *45*, 1378.
13. Fu, Q.; Sanbe, H.; Kagawa, C.; Kunimoto, K. K.; Haginaka, J. *Anal. Chem.* **2003**, *75*, 191.
14. Kempe, H.; Kempe, M. *Macromol. Rapid Commun.* **2004**, *25*, 315.

15. Pérez-Moral, N.; Mayes, A. G. *Anal. Chim. Acta* **2004**, *504*, 15.
16. Yoshimatsu, K.; Reimhult, K.; Krozer, A.; Mosbach, K.; Sode, K.; Ye, L. *Anal. Chim. Acta* **2007**, *584*, 112.
17. Downey, J. S.; Frank, R. S.; Li, W. H.; Stöver, D. H. *Macromolecules* **1999**, *32*, 2838.
18. Sambe, H.; Hoshina, K.; Moaddel, R.; Wainer, I. W.; Haginaka, J. *J. Chromatogr. A* **2006**, *1134*, 88.
19. Priego-Capote, F.; Ye, L.; Shakil, S.; Shamsi, S. A.; Nilsson, S. *Anal. Chem.* **2008**, *80*, 2881.
20. Barahona, F.; Turiel, E.; Cormack, P. A. G.; Martín-Esteban, A. *J. Sep. Sci.* **2011**, *34*, 217.
21. Ho, K. C.; Yeh, W. M.; Tung, T. S.; Liao, J. Y. *Anal. Chim. Acta* **2005**, *542*, 90.
22. Medina-Castillo, A. L.; Mistlberger, G.; Fernandez-Sanchez, J. F.; Segura-Carretero, A.; Klimant, I.; Fernandez-Gutierrez, A. *Macromolecules* **2010**, *43*, 55.
23. Manley, J. B.; Anastas, P. T.; Berkeley, W. C. J. *J. Clean Prod.* **2008**, *16*, 743.
24. Dirion, B.; Cobb, Z.; Schillinger, E.; Andersson, L. I.; Sellergren, B. *J. Am. Chem. Soc.* **2003**, *125*, 15101.
25. Meng, Z.; Chen, W.; Mulchandani, A. *Environ. Sci. Technol.* **2005**, *39*, 8958.
26. Kubo, T.; Hosoya, K.; Nomachi, M.; Tanaka, N.; Kaya, K. *Anal. Bioanal. Chem.* **2005**, *382*, 1698.
27. Caro, E.; Marcé, R. M.; Cormack, P. A. G.; Sherrington, D. C.; Borrull, F. *Anal. Chim. Acta* **2005**, *552*, 81.
28. Cai, W. S.; Gupta, R. B. *Sep. Purif. Technol.* **2004**, *35*, 215.
29. Suedee, R.; Srichana, T.; Chuchome, T.; Kongmark, U. *J. Chromatogr. B* **2004**, *811*, 191.
30. Ni, H. M.; Kawaguchi, H. *J. Polym. Sci. Part A: Polym. Chem.* **2004**, *42*, 2823.
31. Parke, T. V.; Davis, W. W. *Anal. Chem* **1954**, *26*, 642.
32. Langmuir, I. *J. Am. Chem. Soc.* **1918**, *40*, 1361.
33. Weber, T. W.; Chakkravorti, R. K. *AIChE J.* **1974**, *20*, 228.
34. Freundlich, H. M. F. *J. Phys. Chem.* **1906**, *57*, 385.
35. Umpleby, R. J.; Baxter, S. C.; Bode, M.; Berch, J. K.; Shah, R. N.; Shimizu, K. D. *Anal. Chim. Acta* **2001**, *435*, 35.
36. Abramian, L.; El-Rassy, H. *Chem. Eng. J.* **2009**, *150*, 403.
37. Zhang, Z. Y.; Zhang, Z. B.; Fernández, Y.; Menéndez, J. A.; Niu, H.; Peng, J. H.; Zhang, L. B.; Guo, S. H. *Appl. Surf. Sci.* **2010**, *256*, 2569.
38. Mezenner, N. Y.; Bensmaili, A. *Chem. Eng. J.* **2009**, *147*, 87.
39. Ho, Y. S.; McKay, G. *Process. Biochem.* **1999**, *34*, 451.
40. Wu, F. C.; Tseng, R. L.; Juang, R. S. *J. Colloid Interface Sci.* **2005**, *283*, 49.
41. Hu, X. G.; Pan, J. L.; Hu, Y. L.; Huo, Y., Li, G. K. *J. Chromatogr. A* **2008**, *1188*, 97.